

ADAPTIVE FINITE ELEMENT METHODS

LONG CHEN

Adaptive methods are now widely used in the scientific computation to achieve better accuracy with minimum degree of freedom. In this chapter, we shall briefly survey recent progress on the convergence analysis of adaptive finite element methods (AFEMs) for second order elliptic partial differential equations and refer to Nochetto, Siebert and Veerer [14] for a detailed introduction to the theory of adaptive finite element methods.

1. INTRODUCTION TO MESH ADAPTATION

We start with a simple motivation in 1D for the use of adaptive procedures. Given $\Omega = (0, 1)$, a grid $\mathcal{T}_N = \{x_i\}_{i=0}^N$ of Ω

$$0 = x_0 < x_1 < \cdots < x_i < \cdots < x_N = 1$$

and a continuous function $u : \Omega \rightarrow \mathbb{R}$, we consider the problem of approximating u by a piecewise constant function u_N over \mathcal{T}_N . We measure the error in the maximum norm.

Suppose that u is Lipschitz in $[0, 1]$. Consider the approximation

$$u_N(x) := u(x_{i-1}), \text{ for all } x_{i-1} \leq x < x_i.$$

If the grid is quasi-uniform in the sense that $h_i = x_i - x_{i-1} \leq C/N$ for $i = 1, \dots, N$, then it is easy to show that

$$(1) \quad \|u - u_N\|_\infty \leq CN^{-1} \|u'\|_\infty$$

We can achieve the same convergent rate N^{-1} with less smoothness of the function. Suppose $\|u'\|_{L^1} \neq 0$. Let us define a grid distribution function

$$F(x) := \frac{1}{\|u'\|_{L^1}} \int_0^x |u'(t)| dt.$$

Then $F : [0, 1] \rightarrow [0, 1]$ is a non-decreasing function. Let $y_i = i/N, i = 0, \dots, N$ be a uniform grid. We choose x_i such that $F(x_i) = y_i$, see Fig. 1 for an illustration.

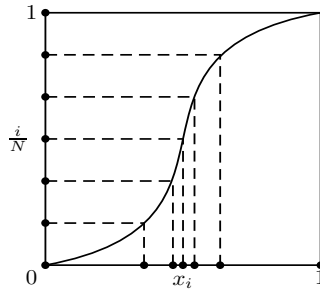


FIGURE 1. A grid distribution function

Then

$$(2) \quad \int_{x_{i-1}}^{x_i} |u'(t)| dt = F(y_i) - F(y_{i-1}) = N^{-1},$$

and

$$|u(x) - u(x_{i-1})| \leq \int_{x_{i-1}}^{x_i} |u'(t)| dt \leq N^{-1} \|u'\|_{L^1},$$

which leads to the estimate

$$(3) \quad \|u - u_N\|_{\infty} \leq CN^{-1} \|u'\|_{L^1}.$$

We use the following example to illustrate the advantage of (3) over (1). Let us consider the function $u(x) = x^r$ with $r \in (0, 1)$. Then $u' \notin L^{\infty}(\Omega)$ but $u' \in L^1(\Omega)$. Therefore we cannot obtain optimal convergent rate on quasi-uniform grids while we could on the correctly adapted grid. For this simple example, one can easily compute when

$$x_i = \left(\frac{i}{N}\right)^{1/r}, \quad \text{for all } 0 \leq i \leq N,$$

estimate (3) will hold on the grid $\mathcal{T}_N = \{x_i\}_{i=0}^N$ which has higher density of grid points near the singularity of u .

In (2), we choose a grid such that an upper bound of the error is equidistributed. This is instrumental for adaptive finite element methods on solving PDEs.

A possible MATLAB code is given below.

```

1 function x = equidistribution(M, x)
2 h = diff(x);
3 F = [0; cumsum(h.*M)];
4 F = F/F(end);
5 y = (0:1/(length(x)-1):1)';
6 x = interp1(F, x, y);

```

Examples of adaptive grids for two functions with singularity are plotted below.

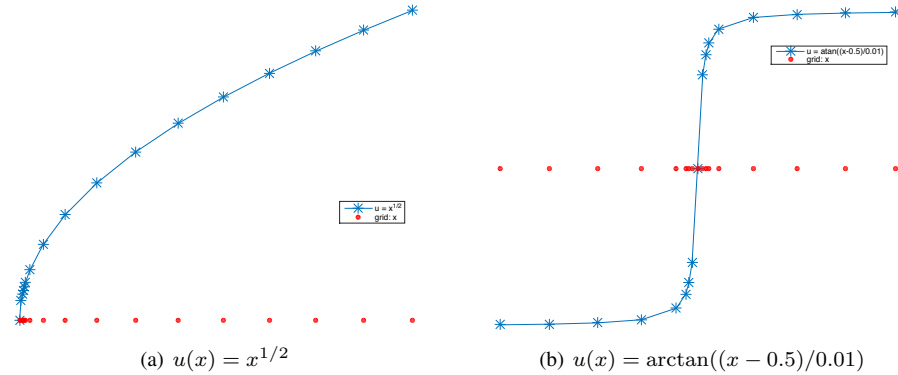


FIGURE 2. Adaptive grids for two functions with singularity.

When applied to numerical solution of PDEs, the function u and its derivatives are unknown. Only an approximated solution to the function u at grid points is available and a good approximation of derivatives or a upper bound of the error should be computed by

a post-processing procedure. Another difficulty is the mesh requirement in two and higher dimensions. The mesh refinement, coarsening, or movement is much more complicated in higher dimensions.

Exercise 1.1. We consider the piecewise linear approximation of a second differentiable function in this exercise.

- (1) When $|f|$ is monotone decreasing, for a positive integer k , prove

$$\frac{1}{(k-1)!} \int_{x_i}^{x_{i+1}} |f(x)|(x-x_i)^{k-1} dx \leq \frac{1}{k!} \left(\int_{x_i}^{x_{i+1}} |f(x)|^{1/k} dx \right)^k.$$

- (2) Let u_I be the nodal interpolation of u on a grid, i.e., u_I is piecewise linear and $u_I(x_i) = u(x_i)$ for all i . Prove that if $|u''(x)|$ is monotone decreasing in (x_{i-1}, x_i) , then for $x \in (x_{i-1}, x_i)$

$$|(u - u_I)(x)| \leq \left(\int_{x_{i-1}}^{x_i} |u''(s)|^{1/2} ds \right)^2.$$

Hint: Apply the inequality in part (1) to the expansion of $u - u_I$ in terms of the barycentric coordinates; see Exercises in Chapter: Introduction to Finite Element Methods.

- (3) Give the condition on the grid distribution and the function such that the following estimate holds and prove your result.

$$\|u - u_I\|_\infty \leq C \|u''\|_{1/2} N^{-2}.$$

2. SINGULARITY AND EQUIDISTRIBUTION

In this section we first present several examples to show that the solution of elliptic equation could have singularity when the domain is concave or the coefficient is discontinuous. We then present a theoretical analysis of equidistribution which leads to optimal order of convergence.

2.1. Lack of Regularity. In FEM, we have obtained a first order convergence of the linear finite element approximation to the Poisson equation

$$(4) \quad -\Delta u = f \quad \text{in } \Omega, \quad u = 0 \quad \text{on } \partial\Omega,$$

provided the solution $u \in H^2(\Omega)$. When the boundary of the domain is smooth or convex and Lipschitz continuous, then $\Delta^{-1}(L^2(\Omega)) \subset H^2(\Omega)$. The requirements of Ω is necessary as shown by the following example.

Consider the domain $\Omega \subset \mathbb{R}^2$ which is defined in a polar coordinate as $\Omega = \{(r, \theta) : 0 < r < 1 \text{ and } 0 < \theta < \frac{\pi}{\beta}\}$ for $1/2 < \beta < \infty$. Obviously if $\beta \geq 1$ then Ω is convex, while if $1/2 < \beta < 1$ then Ω violates the condition of the regularity theory. Set $v = r^\beta \sin(\beta\theta)$ as the imaginary part of the analytic function z^β , i.e., $v = \text{Im}(z^\beta)$. According to the properties of analytic function, we know $\Delta v = 0$. With this fact, it is easy to verify that $u = (1 - r^2)v$ is the solution of the equation (4) with $f = 4(1 + \beta)v \in L^2(\Omega)$.

Now we check the regularity of u . The only possible singularity is at the origin. When r is near 0, the second derivative $D^\alpha u \sim r^{\beta-2}$ for any $|\alpha| = 2$. Considering the integral

$$\int_\Omega |D^\alpha u|^2 dx dy \lesssim \int_0^1 |D^\alpha u|^2 r dr = \int_0^1 r^{2(\beta-2)+1} dr.$$

Therefore $u \in H^2(\Omega)$ if and only if $2(\beta-2)+1 > -1$, i.e., $\beta > 1$. Namely the domain Ω is convex. When β is fixed, by the same calculation, we see $u \in H^s(\Omega)$ for any $s < 1 + \beta$.

If we look for the smoothness in $W^{2,p}(\Omega)$ instead of $H^2(\Omega)$, similar calculation reveals that $\beta > 2(1 - \frac{1}{p})$. For this example, we conclude u belongs to H^s for $1 \leq s < 3/2$ and $W^{2,p}(\Omega)$ for $1 \leq p < 4/3$.

In general, for a polygonal domain Ω with boundary $\partial\Omega$ consisting of a finite number of straight line segments meeting at vertices v_j of interior angles $\alpha_j, j = 1, \dots, M$, let us introduce a polar coordinates (r, θ) at the vertex v_j so that the interior of the wedge is given by $0 < \theta < \alpha_j$ and set $\beta_j = \pi/\alpha_j$, then near v_j the solution u behaves like

$$u(r, \theta) = k_j r^{\beta_j} |\ln r|^{m_j} \sin(\beta_j \theta) + w,$$

where k_j is a constant called the stress intensity factors, $m_j = 0$ unless $\beta_j = 2, 3, \dots$, and $w \in H^2(\Omega)$ is a smooth function. Globally it is easy to see that for any $\epsilon > 0$, $u \in H^{1+\min_j \beta_j - \epsilon}(\Omega)$. In particular, $u \in H^{3/2-\epsilon}(\Omega)$ but $u \notin H^2(\Omega)$ for concave polygonal domains.

For a general elliptic equation

$$(5) \quad -\operatorname{div}(A\nabla u) = f \text{ in } \Omega,$$

the lack of regularity could also come from the discontinuity of the coefficients of A . See the example designed by Kellogg [10] with discontinuous diffusion coefficients in the end of this subsection.

When $u \in H^{1+\epsilon}(\Omega)$ with $\epsilon \in [0, 1]$, in view of the approximation theory, we cannot expect the finite element approximation rate $\|u - u_{\mathcal{T}}\|_{1,\Omega}$ better than h^ϵ if we insist on quasi-uniform grids. To improve the convergence rate for small ϵ , the element size should be adapted to the behavior of the solution. The element size in areas of the domain where the solution is smooth can stay bounded well away from zero, and thus the maximal element size h of a triangulation \mathcal{T} is not a good measure of the approximation rate. For this reason, $N = \#\mathcal{T}$ the number of elements is used, which is also proportional to the number of degree of freedom. Note that $N = \mathcal{O}(h^{-d})$ for quasi-uniform grids.

We include some typical examples below and refer to *i*FEM [8] for numerical evidence that finite element methods based on uniform refined grids will not give optimal order of convergence. But a correctly adapted grid will recovery the optimal convergent order.

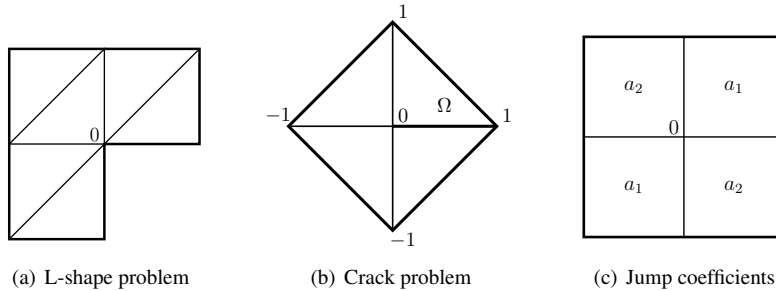


FIGURE 3. Lack of regularity of elliptic equations

L-shape problem. Let $\Omega := (-1, 1)^2 \setminus \{[0, 1] \times (-1, 0]\}$ be a L-shaped domain with a reentrant corner.

$$-\Delta u = 0, \text{ in } \Omega \quad \text{and} \quad u = g \text{ on } \partial\Omega,$$

We choose the Dirichlet boundary condition g such that the exact solution reads

$$u(r, \theta) = r^{\frac{2}{3}} \sin\left(\frac{2}{3}\theta\right),$$

in the polar coordinates.

Crack problem. Let $\Omega = \{|x| + |y| < 1\} \setminus \{0 \leq x \leq 1, y = 0\}$ with a crack and the solution u satisfies the Poisson equation

$$-\Delta u = f, \text{ in } \Omega \quad \text{and} \quad u = u_D \text{ on } \Gamma_D,$$

where $f = 1$, $\Gamma_D = \partial\Omega$. We choose u_D such that the exact solution u in the polar coordinates is

$$u(r, \theta) = r^{\frac{1}{2}} \sin\left(\frac{\theta}{2}\right) - \frac{1}{4}r^2.$$

Jump coefficients problem. Consider the partial differential equation (5) with $\Omega = (-1, 1)^2$ and the coefficient matrix A is piecewise constant: in the first and third quadrants, $A = a_1 I$; in the second and fourth quadrants, $A = a_2 I$. For $f = 0$, the exact solution in the polar coordinates has been chosen to be $u(r, \theta) = r^\gamma \mu(\theta)$, where

$$\mu(\theta) = \begin{cases} \cos\left(\left(\frac{\pi}{2} - \sigma\right)\gamma\right) \cos\left(\left(\theta - \frac{\pi}{2} + \rho\right)\gamma\right) & \text{if } 0 \leq \theta \leq \frac{\pi}{2}, \\ \cos(\rho\gamma) \cos\left(\left(\theta - \pi + \sigma\right)\gamma\right) & \text{if } \frac{\pi}{2} \leq \theta \leq \pi, \\ \cos(\sigma\gamma) \cos\left(\left(\theta - \pi - \rho\right)\gamma\right) & \text{if } \pi \leq \theta \leq \frac{3\pi}{2}, \\ \cos\left(\left(\frac{\pi}{2} - \rho\right)\gamma\right) \cos\left(\left(\theta - \frac{3\pi}{2} - \sigma\right)\gamma\right) & \text{if } \frac{3\pi}{2} \leq \theta \leq 2\pi, \end{cases}$$

and the constants

$$\gamma = 0.1, \quad \rho = \pi/4, \quad \sigma = -14.9225565104455152,$$

and

$$a_1 = 161.4476387975881, \quad a_2 = 1.$$

For this example, we see

$$u \in H^{1+\gamma}(\Omega).$$

One can construct more singular function by choosing arbitrary small γ ; see Kellogg [10].

2.2. Equidistribution. The equidistribution principle has been widely used in the all adaptive finite element algorithms. But a theoretical justification of this principle is very difficult to be made precise. One early justification of this approach is due to Babuška and Rheinboldt [1] and they provide a heuristic asymptotic analysis. In this section, we will illustrate the equidistribution principle in a more elementary fashion. Through our simple theoretical analysis, we will see the equidistribution is indeed needed for optimal error control, but on the other hand, we will show optimal convergent rate can still be maintained when equidistribution are much relaxed.

We shall consider a simple elliptic boundary value problem

$$(6) \quad -\Delta u = f \text{ in } \Omega, \quad u = 0 \text{ on } \partial\Omega,$$

where, for simplicity, we assume Ω is a polygon and is partitioned by a shape regular conforming triangulation \mathcal{T}_N with N number of triangles. Let $\mathcal{V}_N \subset H_0^1(\Omega)$ be the corresponding continuous piecewise linear finite element space associated with this triangulation \mathcal{T}_N .

A finite element approximation of the above problem is to find $u_N \in \mathcal{V}_N$ such that

$$(7) \quad a(u_N, v_N) = (f, v_N) \quad \forall v_N \in \mathcal{V}_N,$$

where

$$a(u, v) = \int_{\Omega} \nabla u \cdot \nabla v \, dx, \text{ and } (f, v) = \int_{\Omega} f v \, dx.$$

For this problem, it is well known that for a fixed finite element space \mathcal{V}_N

$$(8) \quad |u - u_N|_{1, \Omega} = \inf_{v_N \in \mathcal{V}_N} |u - v_N|_{1, \Omega}.$$

We then present a H^1 error estimate for linear triangular element interpolation in two dimensions. We note that in two dimensions, the following two embeddings are both valid:

$$(9) \quad W^{2,1}(\Omega) \subset W^{1,2}(\Omega) \equiv H^1(\Omega) \text{ and } W^{2,1}(\Omega) \subset C(\bar{\Omega}).$$

Given $u \in W^{2,1}(\Omega)$, let u_I be the linear nodal value interpolant of u on \mathcal{T}_N . For any triangle $\tau \in \mathcal{T}_N$, thanks to (9) and the assumption that τ is shape-regular, we have

$$|u - u_I|_{1, \tau} \lesssim |u|_{2,1, \tau}.$$

As a result,

$$|u - u_I|_{1, \Omega}^2 \lesssim \sum_{\tau \in \mathcal{T}_N} |u|_{2,1, \tau}^2.$$

To minimize the error, we can try to minimize the right hand side. By Cauchy-Schwarz inequality,

$$|u|_{2,1, \Omega} = \sum_{\tau \in \mathcal{T}_N} |u|_{2,1, \tau} \leq \left(\sum_{\tau \in \mathcal{T}_N} 1 \right)^{1/2} \left(\sum_{\tau \in \mathcal{T}_N} |u|_{2,1, \tau}^2 \right)^{1/2} = N^{1/2} \left(\sum_{\tau \in \mathcal{T}_N} |u|_{2,1, \tau}^2 \right)^{1/2}.$$

Thus, we have the following lower bound:

$$(10) \quad \left(\sum_{\tau \in \mathcal{T}_N} |u|_{2,1, \tau}^2 \right)^{1/2} \geq N^{-1/2} |u|_{2,1, \Omega}.$$

The equality holds if and only if

$$(11) \quad |u|_{2,1, \tau} = \frac{1}{N} |u|_{2,1, \Omega}.$$

The condition (11) is hard to be satisfied in general. But we can considerably relax this condition to ensure the lower bound estimate (10) is still achieved asymptotically. The relaxed condition is as follows:

$$(12) \quad |u|_{2,1, \tau} \leq \kappa_{\tau, N} |u|_{2,1, \Omega}$$

and

$$(13) \quad \sum_{\tau \in \mathcal{T}_N} \kappa_{\tau, N}^2 \leq c_1 N^{-1}.$$

When the above two inequalities hold, we have

$$|u - u_I|_{1, \Omega} \lesssim N^{-1/2} |u|_{2,1, \Omega}.$$

In summary, we have the following theorem.

Theorem 2.1. *If \mathcal{T}_N is a triangulation with at most N triangles and satisfying (12) and (13), then*

$$(14) \quad |u - u_N|_1 \leq |u - u_I|_{1, \Omega} \lesssim N^{-1/2} |u|_{2,1, \Omega}.$$

In the above analysis, we see how equidistribution principle plays an important role in achieving asymptotically optimal accuracy for adaptive grids. We would like to further elaborate that, in the current setting, equidistribution is indeed a sufficient condition for optimal error, but by no means this has to be a necessary condition. Namely the equidistribution principle can be severely violated but asymptotically optimal error estimates can still be maintained. For example, the following mild violation of this principle is certainly acceptable:

$$(15) \quad |u|_{2,1,\tau} \leq \frac{c}{N} |u|_{2,1,\Omega}.$$

In fact, this condition can be more significantly violated on a finitely many elements $\{\tau\}$

$$(16) \quad |u|_{2,1,\tau} \leq \frac{c}{\sqrt{N}} |u|_{2,1,\Omega}.$$

It is easy to see if a bounded number of elements satisfy (16) and the rest satisfy (15), the estimate (13) is satisfied and hence the optimal error estimate (14) is still valid.

As we can see that the condition (16) is a very serious violation of equidistribution principle, nevertheless, as long as such violations do not occur on too many elements, asymptotically optimal error estimates are still valid. This simple observation is important from both theoretical and practical points of view. The marking strategy proposed by [9] may also be interpreted in this way in its relationship with equidistribution principle.

As it turns out, rigorously speaking, we need a slightly stronger assumption on u (namely smoother than $W^{2,1}(\Omega)$), for example, $u \in W^{2,p}(\Omega)$ ¹ for some $p > 1$. This assumption is true for most practical domains; see the discussion in the previous subsection. More precisely, for any $p > 1$, any N , we have a constructive algorithm [3] to find a shape-regular triangulation \mathcal{T}_N with $\mathcal{O}(N)$ elements such that

$$|u|_{2,1,\tau} \leq c_0 N^{-1} |u|_{2,p,\Omega}.$$

As a result, since $|u - u_{\mathcal{T}}|_{1,\Omega} \leq |u - u_I|_{1,\Omega}$, we have the following error estimate

$$(17) \quad |u - u_{\mathcal{T}}|_{1,\Omega} \lesssim N^{-1/2} |u|_{2,p,\Omega}.$$

which is asymptotically best possible for an isotropic triangulation with $\mathcal{O}(N)$ elements. Recent works have shown that the estimate (17) can be practically realized [6, 7, 13, 18] by using appropriate *a posteriori* error estimates below.

3. NEWEST VERTEX BISECTION

In this section we shall give a brief introduction of the newest vertex bisection. We refer to [12, 19, 6] for detailed description of the newest vertex bisection refinement procedure and especially [6] for the control of the number of elements added by the completion process.

We first recall two important properties of triangulations. A triangulation \mathcal{T}_h (also indicated by mesh or grid) of $\Omega \subset \mathbb{R}^2$ is a decomposition of Ω into a set of triangles. It is called *conforming* if the intersection of any two triangles τ and τ' in \mathcal{T}_h either consists of a common vertex x_i , edge E or empty. An edge of a triangle is called *non-conforming* if there is a vertex in the interior of that edge and that interior vertex is called *hanging node*. See Fig. 3 (b) for an example of non-conforming triangles and hanging nodes. We would like to keep the conformity of the triangulations.

¹it actually suffices if $M(\nabla^2 u) \in L^1(\Omega)$, where $M(f)$ is the Hardy-Littlewood maximal function of f

A triangulation \mathcal{T}_h is *shape regular* if

$$(18) \quad \max_{\tau \in \mathcal{T}_h} \frac{\text{diam}(\tau)^2}{|\tau|} \leq \sigma$$

where $\text{diam}(\tau)$ is the diameter of τ and $|\tau|$ is the area of τ . A sequence of triangulation $\{\mathcal{T}_k, k = 0, 1, \dots\}$ is called *uniform shape regular* if σ in (18) is independent with k .

The shape regularity of triangulations assures that angles of the triangulation remains bounded away from 0 and π which is important to control the interpolation error in H^1 norm and the condition number of the stiffness matrix. We also want to keep this property of the triangulations.

After we marked a set of triangles to be refined, we need to carefully design the rule for dividing the marked triangles such that the refined mesh is still conforming and shape regular. Such refinement rules include red and green refinement [4], longest edge bisection [16, 15] and newest vertex bisection [17]. We shall restrict ourself to the newest vertex bisection method since it will produce nested finite element spaces and relatively easier to generalize to high dimensions.

Given an initial shape regular triangulation \mathcal{T}_0 of Ω , we assign to each $\tau \in \mathcal{T}_0$ exactly one vertex called *the newest vertex*. The opposite edge of the newest vertex is called *refinement edge*. One such initial labeling is to use the longest edge of each triangle (with a tie breaking scheme for edges of equal length). The rule of the newest vertex bisection includes:

- (1) a triangle is divided to two new children triangles by connecting the newest vertex to the midpoint of the refinement edge;
- (2) the new vertex created at a midpoint of a refinement edge is assigned to be the newest vertex of the children.

It is easy to verify that all the descendants of an original triangle fall into four similarity classes (see Figure 1) and hence the angles are bounded away from 0 and π and all triangulations refined from \mathcal{T}_0 using newest vertex bisection forms a shape regular class of triangulations.

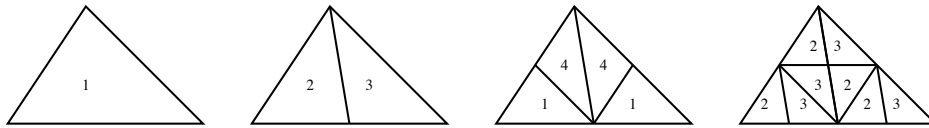


FIGURE 4. Four similarity classes of triangles generated by the newest vertex bisection

Remark 3.1. If we always chose the longest edge as the refinement edge, this is known as the longest edge bisection. It is possible to verify the uniformly shape regularity of the produced mesh by using the geometry property; see [16, 15].

The triangulation obtained by the newest vertex might have hanging nodes. We have to make additional subdivisions to eliminate the hanging nodes, i.e., complete the new partition. The completion should also follow the bisection rules to keep the shape regularity; see Figures below for an illustration of the completion procedure.

Let M denotes the set of triangles to be refined. A standard iterative algorithm of the completion is the following.

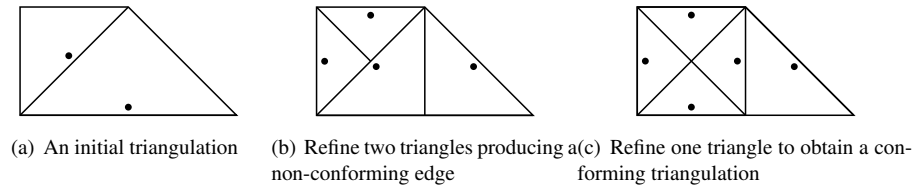


FIGURE 5. An illustration of the completion procedure. The dot indicates the refinement edge of each triangle.

```

1 function T = completion(T,M)
2 while M is not empty
3     Update T by bisecting each triangle in M;
4     Let now M be the set of non-conforming triangles.
5 end

```

We need to show the `while` loop will terminate. For two dimensional triangulation, this is easy. Let us denote the uniform bisection of \mathcal{T} as $D(\mathcal{T})$, i.e., every triangle is bisected into two. Note that $D(\mathcal{T})$ may not be conforming; see Fig 3 (b). But $D^2(\mathcal{T})$, which corresponds to bisecting every triangle twice, is always conforming since middle points of all edges are added from \mathcal{T} to $D^2(\mathcal{T})$. We consider the completion procedure as a procedure of splitting edges. The edges split during the completion procedure is a subset of the edge set of \mathcal{T} which is finite and thus the completion will terminate.

If we ask more than the termination of the completion process and want to control the number of elements refined due to the completion, we have to carefully assign the newest vertex for the initial partition \mathcal{T}_0 . A triangle is called *compatible divisible* if its refinement edge is either the refinement edge of the triangle that shares that edge or an edge on the boundary. A triangulation \mathcal{T} is called *compatible divisible* or *compatible labeled* if every triangle is compatible divisible. Mitchell [11] proved that for any conforming triangulation \mathcal{T} , there exists a compatible labeling. Biedl et al. [5] give an $\mathcal{O}(N)$ algorithm to find a compatible labeling for a triangulation with N elements.

Binev, Dahmen and DeVore [6] show that if \mathcal{M} is the collection of all triangles marked in going from a conforming divisible triangulation \mathcal{T}_0 to \mathcal{T}_k then

$$(19) \quad \#\mathcal{T}_k \leq \#\mathcal{T}_0 + C\#\mathcal{M},$$

where $\#A$ denotes the cardinality of the set A . That is the number of addition triangles refined in the completion procedure is bounded by the number of marked triangles in the l^1 sense. The inequality (19) cannot be true in the l^∞ sense. Refine one marked triangle could trigger a sequence of triangles with length equals to its generation in the completion procedure; see the following figure. The inequality (19) is crucial for the optimality of adaptive finite element methods; see [6, 7].

We conclude this section by a remark that the bisection or the regular refinement in three and higher dimensions is much more involved. The theoretical proof of the shape regularity, the termination of completion, and the control of number of elements added in the completion requires more careful combinatorial study; see [14].

4. RESIDUAL TYPE A POSTERIOR ERROR ESTIMATE

In this section we consider the linear finite element approximation of the Poisson

$$(20) \quad -\Delta u = f \text{ in } \Omega, \quad u = 0 \text{ on } \partial\Omega,$$

and shall derive a residual type *a posteriori* error estimate of the error $|u - u_{\mathcal{T}}|_{1,\Omega}$. [Other types of a posteriori error estimator include: recovery type; solving local problem; solving a dual problem; superconvergence result.](#)

4.1. A local and stable quasi-interpolation. To define a function in the linear finite element space $\mathcal{V}_{\mathcal{T}}$, we only need to assigned the value at interior vertices. For a vertex $x_i \in \mathcal{N}(\mathcal{T})$, recall that Ω_i consists of all simplexes sharing this vertex and for an element $\Omega_{\tau} = \cup_{x_i \in \tau} \Omega_i$. Instead of using nodal values of the object function, we can use its integral over Ω_i .

For an interior vertex x_i , we define a constant function on Ω_i by $A_i u = |\Omega_i|^{-1} \int_{\Omega_i} u(x) dx$. To incorporate the boundary condition, when $x_i \in \partial\Omega$, we define $A_i u = 0$. We then define the averaged interpolation $\Pi_{\mathcal{T}} : L^1 \mapsto \mathcal{V}_{\mathcal{T}}$ by

$$\Pi_{\mathcal{T}} u = \sum_{x_i \in \mathcal{N}(\mathcal{T})} A_i(u) \varphi_i.$$

Lemma 4.1. *For $u \in H^1(\Omega_{\tau})$, we have the error estimate*

$$\|u - \Pi_{\mathcal{T}} u\|_{0,\tau} \lesssim h_{\tau} |u|_{1,\Omega_{\tau}}.$$

Proof. For interior vertices, we use average type Poincaré inequality, to obtain

$$(21) \quad \|u - A_i u\|_{0,\Omega_i} \leq C h_{\tau} |u|_{1,\Omega_i},$$

and for boundary vertices, we use Poincaré-Friedrichs since then $u|_{\partial\Omega_i \cap \partial\Omega} = 0$ and the \mathbb{R}^{d-1} Lebesgue measure of the set $\partial\Omega_i \cap \partial\Omega$ is non-zero. The constant C in the equality (21) can be chosen as one independent with Ω_i since the mesh is shape regular. Then we use the partition of unity $\sum_{i=1}^{d+1} \varphi_i = 1$ restricted to one element τ to write

$$\begin{aligned} \int_{\tau} |u - \Pi_{\mathcal{T}} u|^2 &= \int_{\tau} \left| \sum_{i=1}^{d+1} (u - A_i u) \varphi_i \right|^2 dx \lesssim \sum_{i=1}^{d+1} \int_{\Omega_i} |u - A_i u|^2 dx \\ &\lesssim h_{\tau} \sum_{i=1}^{d+1} \int_{\Omega_i} |\nabla u|^2 dx \lesssim C h_{\tau}^2 \int_{\Omega_{\tau}} |\nabla u|^2 dx. \end{aligned}$$

□

We now prove that $\Pi_{\mathcal{T}}$ is stable in H^1 norm. Let us introduce another average operator A_{τ} : the L^2 projection to the piecewise constant function spaces on \mathcal{T}_h : $(A_{\tau} u)|_{\tau} = |\tau|^{-1} \int_{\tau} u(x) dx$.

Lemma 4.2. *For $u \in H^1(\Omega_{\tau})$, we have the stability*

$$|\Pi_{\mathcal{T}} u|_{1,\tau} \lesssim |u|_{1,\Omega_{\tau}}.$$

Proof. Using Poincaré inequality it is easy to see

$$\|u - A_{\tau} u\|_{0,\tau} \lesssim h_{\tau} |u|_{1,\tau}.$$

We use the inverse inequality and first order approximation property of A_τ and Π_τ to obtain

$$\begin{aligned} |\Pi_\tau u|_{1,\tau} &= |\Pi_\tau u - A_\tau u|_{1,\tau} \leq h_\tau^{-1} \|\Pi_\tau u - A_\tau u\|_{0,\tau} \\ &\leq h_\tau^{-1} \left(\|u - \Pi_\tau u\|_{0,\tau} + \|u - A_\tau u\|_{0,\tau} \right) \lesssim |u|_{1,\Omega_\tau}. \end{aligned}$$

□

Theorem 4.3. *For $u \in H^1(\Omega)$, the quasi-interpolant $\Pi_\tau u$ satisfies*

$$\left(\sum_{\tau \in \mathcal{T}} \|h^{-1}(u - \Pi_\tau u)\|_{0,\tau}^2 + \|\nabla(u - \Pi_\tau u)\|_{0,\tau}^2 \right)^{1/2} \lesssim |u|_{1,\Omega}.$$

4.2. Upper bound. The equidistribution principle suggested us to equidistribute the quantity $|u|_{2,1,\tau}$. It is, however, not computable since u is unknown. One may want to approximate it by $|u_\tau|_{2,1,\tau}$. For linear finite element function u_τ , we have $|u_\tau|_{2,1,\tau} = 0$ and thus no information of $|u|_{2,1,\tau}$ will be obtained in this way. More rigorously, the derivative of the piecewise constant vector function ∇u_τ will be delta distributions on edges with magnitude as the jump of ∇u_τ across the edge. On the other hand, $\Delta u \in L^2(\Omega)$ implies $\nabla u \in H(\text{div}; \Omega)$, i.e., $\nabla u \cdot n_e$ is continuous at an edge e where n_e is a unit norm vector of e . For the finite element approximation $u_\tau \in \mathcal{V}_\tau$, it is easy to see $\nabla u_\tau \cdot n_e$ is not continuous (although the tangential derivative $\nabla u_\tau \cdot t_e$ is). The discontinuity of norm derivative across edges can be used to measure the error $\nabla u - \nabla u_\tau$.

More precisely, let \mathcal{E}_τ denote the set of all interior edges, for each interior edge $e \in \mathcal{E}_\tau$, we fix a unit norm vector n_e . Let τ_1 and τ_2 be two triangles sharing the edge e . The jump of flux across e is defined as

$$[\nabla u_\tau \cdot n_e] = \nabla u_\tau \cdot n_e|_{\tau_1} - \nabla u_\tau \cdot n_e|_{\tau_2}.$$

We define h as a piecewise constant function on \mathcal{T} , that is for each element $\tau \in \mathcal{T}$,

$$(22) \quad h|_\tau = h_\tau = |\tau|^{1/2}.$$

We also define a piecewise constant function on \mathcal{E}_τ as

$$(23) \quad h|_e = h_e := (h_{\tau_1} + h_{\tau_2})/2,$$

where $e = \tau_1 \cap \tau_2$ is the common edge of two triangles. We provide a posterior error estimate for the Poisson equation with homogenous Dirichlet boundary condition below and refer to [19] for general elliptic equations and mixed boundary conditions.

Theorem 4.4. *For a given triangulation \mathcal{T} , let u_τ be the linear finite element approximation of the solution u of the Poisson equation. Then there exists a constant $C_1 > 0$ depending only on the shape regularity of \mathcal{T} such that*

$$(24) \quad |u - u_\tau|_1 \leq C_1 \left(\sum_{\tau \in \mathcal{T}} \|hf\|_{0,\tau}^2 + \sum_{e \in \mathcal{E}_\tau} \|h^{1/2}[\nabla u_\tau \cdot n_e]\|_{0,e}^2 \right)^{1/2}.$$

Proof. For any $w \in H_0^1(\Omega)$ and any $w_{\mathcal{T}} \in \mathcal{V}_{\mathcal{T}}$, we have

$$\begin{aligned}
& a(u - u_{\mathcal{T}}, w) \\
&= a(u - u_{\mathcal{T}}, w - w_{\mathcal{T}}) \\
&= \sum_{\tau \in \mathcal{T}} \int_{\tau} \nabla(u - u_{\mathcal{T}}) \cdot \nabla(w - w_{\mathcal{T}}) \, dx \\
&= \sum_{\tau \in \mathcal{T}} \int_{\tau} -\Delta(u - u_{\mathcal{T}})(w - w_{\mathcal{T}}) \, dx + \sum_{\tau \in \mathcal{T}} \int_{\partial\tau} \nabla(u - u_{\mathcal{T}}) \cdot n(w - w_{\mathcal{T}}) \, dS \\
&= \sum_{\tau \in \mathcal{T}} \int_{\tau} f(w - w_{\mathcal{T}}) \, dx + \sum_{e \in \mathcal{E}_h} \int_e [\nabla u_{\mathcal{T}} \cdot n_e](w - w_{\mathcal{T}}) \, dS \\
&\leq \sum_{\tau \in \mathcal{T}} \|hf\|_{0,\tau} \|h^{-1}(w - w_{\mathcal{T}})\|_{0,\tau} + \sum_{e \in \mathcal{E}_h} \|h^{1/2}[\nabla u_{\mathcal{T}} \cdot n_e]\|_{0,e} \|h^{-1/2}(w - w_{\mathcal{T}})\|_{0,e} \\
&\lesssim \left(\sum_{\tau \in \mathcal{T}} \|hf\|_{0,\tau}^2 + \sum_{e \in \mathcal{E}_{\mathcal{T}}} \|h^{-1/2}[\nabla u_{\mathcal{T}} \cdot n_e]\|_{0,e}^2 \right)^{1/2} \\
&\quad \left(\sum_{\tau \in \mathcal{T}} \|h^{-1}(w - w_{\mathcal{T}})\|_{0,\tau}^2 + \|\nabla(w - w_{\mathcal{T}})\|_{0,\tau}^2 \right)^{1/2}.
\end{aligned}$$

In the last step, we have used the trace theorem with the scaling argument to get

$$\|w - w_{\mathcal{T}}\|_{0,e} \lesssim h_{\tau}^{-1/2} \|w - w_{\mathcal{T}}\|_{0,\tau} + h_{\tau}^{1/2} \|\nabla(w - w_{\mathcal{T}})\|_{0,\tau}.$$

Now chose $w_{\mathcal{T}} = \Pi_{\mathcal{T}}w$ by the quasi-interpolation operator introduced in Theorem 4.3, we have

$$(25) \quad \left(\sum_{\tau \in \mathcal{T}} \|h^{-1}(w - w_{\mathcal{T}})\|_{0,\tau}^2 + \|\nabla(w - w_{\mathcal{T}})\|_{0,\tau}^2 \right)^{1/2} \lesssim |w|_{1,\Omega}.$$

Then we end with

$$|u - u_{\mathcal{T}}|_1 = \sup_{w \in H_0^1(\Omega)} \frac{a(u - u_{\mathcal{T}}, w)}{|w|_1} \lesssim \left(\sum_{\tau \in \mathcal{T}} \|hf\|_{0,\tau}^2 + \sum_{e \in \mathcal{E}_{\mathcal{T}}} \|h^{1/2}[\nabla u_{\mathcal{T}} \cdot n_e]\|_{0,e}^2 \right)^{1/2}.$$

□

To guide the local refinement, we need to have an element-wise (or edge-wise) error indicator. For any $\tau \in \mathcal{T}$ and any $v_{\mathcal{T}} \in \mathcal{V}_{\mathcal{T}}$, we define

$$(26) \quad \eta(v_{\mathcal{T}}, \tau) = \left(\|hf\|_{0,\tau}^2 + \sum_{e \in \partial\tau} \|h^{1/2}[\nabla v_{\mathcal{T}} \cdot n_e]\|_{0,e}^2 \right)^{1/2}.$$

For a subset $\mathcal{M}_{\mathcal{T}} \subseteq \mathcal{T}$, we define

$$\eta(v_{\mathcal{T}}, \mathcal{M}_{\mathcal{T}}) = \left[\sum_{\tau} \eta^2(v_{\mathcal{T}}, \tau) \right]^{1/2}.$$

With these notation, the upper bound (24) can be simply written as

$$(27) \quad |u - u_{\mathcal{T}}|_{1,\Omega} \leq C_1 \eta(u_{\mathcal{T}}, \mathcal{T}).$$

Remark 4.5. The local version of the upper bound (27)

$$|u - u_{\mathcal{T}}|_{1,\tau} \leq C_1 \eta(u_{\mathcal{T}}, \tau)$$

does not hold in general.

4.3. Lower bound. We shall derive a lower bound of the error estimator η through the following exercises. The technique is developed by Verfürth [19] and known as bubble functions. Let u be the solution of Poisson equation $-\Delta u = f$ with homogeneous Dirichlet boundary condition and $u_{\mathcal{T}}$ be the linear finite element approximation of u based on a shape regular and conforming triangulation \mathcal{T} .

Exercise 4.6. (1) For a triangle τ , we denote $V_{\tau} = \{f_{\tau} \in L^2(\tau) \mid f_{\tau} = \text{constant}\}$ equipped with L^2 inner product. Let $\lambda_i(x)$, $i = 1, 2, 3$ be the barycenter coordinates of $x \in \tau$, and let $b_{\tau} = \lambda_1 \lambda_2 \lambda_3$ be the bubble function on τ . We define $B_{\tau} f_{\tau} = f_{\tau} b_{\tau}$.

Prove that $B_{\tau} : V_{\tau} \mapsto V = H_0^1(\Omega)$ is bounded in L^2 and H^1 norm:

$$\|B_{\tau} f_{\tau}\|_{0,\tau} = C \|f_{\tau}\|_{0,\tau}, \quad \text{and} \quad \|\nabla(B_{\tau} f_{\tau})\|_{0,\tau} \lesssim h_{\tau}^{-1} \|f_{\tau}\|_{0,\tau}.$$

(2) Using (1) to prove that

$$\|h f_{\tau}\|_{0,\tau} \lesssim |u - u_{\mathcal{T}}|_{1,\tau} + \|h(f - f_{\tau})\|_{0,\tau}.$$

(3) For an interior edge e , we define $V_e = \{g_e \in L^2(E) \mid g_e = \text{constant}\}$. Suppose e has end points x_i , and x_j , we define $b_e = \lambda_i \lambda_j$ and $B_e : V_e \mapsto V$ by $B_e g_e = g_e b_e$.

Let ω_e denote two triangles sharing e . Prove that

- (a) $\|g_e\|_{0,e} = C \|B_e g_e\|_{0,e}$,
- (b) $\|B_e g_e\|_{0,\omega_e} \lesssim h_e^{1/2} \|g_e\|_{0,e}$ and,
- (c) $\|\nabla(B_e g_e)\|_{0,\omega_e} \lesssim h_e^{-1/2} \|g_e\|_{0,e}$.

(4) Using (3) to prove that

$$\|h^{1/2} [\nabla u_{\mathcal{T}} \cdot n_e]\|_{0,e} \lesssim \|h f\|_{0,\omega_e} + |u - u_{\mathcal{T}}|_{1,\omega_e}.$$

(5) Using (1) and (4) to prove the lower bound of the error estimator. There exists a constant C_2 depending only on the shape regularity of the triangulation such that for any piecewise constant approximation f_{τ} of $f \in L^2$,

$$C_2 \eta^2(u_{\mathcal{T}}, \mathcal{T}) \leq |u - u_{\mathcal{T}}|_{1,\Omega}^2 + \sum_{\tau \in \mathcal{T}_h} \|h(f - f_{\tau})\|_{\tau}^2.$$

5. CONVERGENCE

Standard adaptive finite element methods (AFEM) based on the local mesh refinement can be written as loops of the form

(28) **SOLVE** \rightarrow **ESTIMATE** \rightarrow **MARK** \rightarrow **REFINE**.

Starting from an initial triangulation \mathcal{T}_0 , to get \mathcal{T}_{k+1} from \mathcal{T}_k we first solve the equation to get u_k based on \mathcal{T}_k (the indices of second order like $u_{\mathcal{T}_k}$ will be contracted as u_k). The error is estimated using u_k and \mathcal{T}_k and used to mark a set of triangles in \mathcal{T}_k . Marked triangles and possible more neighboring triangles are refined in such a way that the triangulation is still shape regular and conforming.

5.1. Algorithm. The step **SOLVE** is discussed in Chapter: Iterative method, where efficient iterative methods including multigrid and conjugate gradient methods is studied in detail. Here we assume that the solutions of the finite dimensional problems can be solved to any accuracy efficiently.

The *a posteriori* error estimators are an essential part of the **ESTIMATE** step. We have given one in the previous section and will discuss more in the next section.

The *a posteriori* error estimator is split into local error indicators and they are then employed to make local modifications by dividing the elements whose error indicator is large and possibly coarsening the elements whose error indicator is small. The way we mark these triangles influences the efficiency of the adaptive algorithm. The traditional maximum marking strategy proposed in the pioneering work of Babuška and Vogelius [2] is to mark triangles τ^* such that

$$\eta(u_{\mathcal{T}}, \tau^*) \geq \theta \max_{\tau \in \mathcal{T}} \eta(u_{\mathcal{T}}, \tau), \quad \text{for some } \theta \in (0, 1).$$

Such marking strategy is designed to evenly equi-distribute the error. Based our relaxation of the equidistribution principal, we may leave some exceptional elements and focus on the overall amounts of the error. This leads to the bulk criterion firstly proposed by Dörfler [9] in order to prove the convergence of the local refinement strategy. With such strategy, one defines the marking set $\mathcal{M}_{\mathcal{T}} \subset \mathcal{T}$ such that

$$(29) \quad \eta^2(u_{\mathcal{T}}, \mathcal{M}_{\mathcal{T}}) \geq \theta \eta^2(u_{\mathcal{T}}, \mathcal{T}), \quad \text{for some } \theta \in (0, 1).$$

We shall use Dörfler marking strategy in the proof.

After choosing a set of marked elements, we need to carefully design the rule for dividing the marked triangles such that the mesh obtained by this dividing rule is still conforming and shape regular. Such refinement rules include red and green refinement [4], longest refinement [16, 15], and newest vertex bisection [17, 12]. In addition we also would like to control the number of elements added to ensure the optimality of the refinement. To this end we shall use the newest vertex bisection discussed in the previous section.

Let us summarize AFEM in the following subroutine:

```

1  [uJ, TJ] = AFEM (T1, f, tol, θ)
2  % AFEM compute an approximation uJ by adaptive finite element methods
3  % Input: T1 an initial triangulation; f data; tol <<1 tolerance; θ ∈ (0,1)
4  % Output: uJ linear finite element approximation; TJ the finest mesh
5  η = 1, k = 0;
6  while η ≥ tol
7      k = k + 1;
8      SOLVE Poisson equation on Tk to get the solution uk;
9      ESTIMATE the error by η = η(uk, Tk);
10     MARK a set Mk ⊂ Tk with minimum number such that η2(uk, Mk) ≥ θ η2(uk, Tk);
11     REFINED τ ∈ Mk and necessary triangles to a conforming triangulation Tk+1;
12 end
13 uJ = uk; TJ = Tk;

```

5.2. Contraction between two levels. We shall prove the convergence of AFEM by showing the contraction of the total error between two levels. That is

$$(30) \quad |u - u_{k+1}|_1^2 + \alpha \eta^2(u_{k+1}, \mathcal{T}_{k+1}) \leq \delta [|u - u_k|_1^2 + \alpha \eta^2(u_k, \mathcal{T}_k)].$$

One may wonder why the error and the error estimator is considered together. Can we prove the reduction of error itself? By the orthogonality, one can easily conclude the error

is non-increasing, i.e.

$$|u - u_{k+1}|_1 \leq |u - u_k|_1.$$

The equality could hold if the refinement did not introduce interior nodes for triangles and edges; see Example 3.6 and 3.7 in [13]. A close look reveals that when the solution does not change, the error estimator η will be reduced by a factor less than one due to the change of mesh size and the Dörfler marking strategy.

To prove (30) let us begin with the following properties of the error estimator and error in consecutive levels \mathcal{T}_k and \mathcal{T}_{k+1} .

Lemma 5.1. *Given a $\theta \in (0, 1)$, let \mathcal{T}_{k+1} be a conforming and shape regular triangulation which is refined from a conforming and shape regular triangulation \mathcal{T}_k using Dörfler marking strategy (29). Let u_{k+1} and u_k be solutions of (4) in \mathcal{V}_{k+1} and \mathcal{V}_k , respectively. Then we have*

- (1) *orthogonality:* $|u - u_{k+1}|_1^2 = |u - u_k|_1^2 - |u_{k+1} - u_k|_1^2$;
- (2) *upper bound:* $|u - u_k|_1^2 \leq C_1 \eta^2(u_k, \mathcal{T}_k)$ for some constant C_1 depending only on the shape regularity of \mathcal{T} ;
- (3) *continuity of error estimator:* for any $\epsilon > 0$, there exists a constant C_ϵ such that

$$\eta^2(u_{k+1}, \mathcal{T}_{k+1}) \leq (1 + \epsilon) \eta^2(u_k, \mathcal{T}_{k+1}) + C_\epsilon |u_{k+1} - u_k|_1^2;$$
- (4) *contraction of error estimator:* $\eta^2(u_k, \mathcal{T}_{k+1}) \leq \rho \eta^2(u_k, \mathcal{T}_k)$ for some $\rho \in (0, 1)$ depending only on the shape regularity of \mathcal{T}_k and the parameter θ used in the Dörfler marking strategy.

Proof. (1) is trivial since u_{k+1} is the H^1 projection and $u_{k+1} - u_k \in \mathcal{V}_{k+1}$ by the nestness of \mathcal{T}_k and \mathcal{T}_{k+1} . (2) has been proved in the previous section.

We now prove (3). The part contains element-wise residual $\|hf\|$ is unchanged since we do not change the triangulation. For each $e \in \mathcal{E}_\mathcal{T}$, let $\tau \in \mathcal{T}$ such that $e \in \partial\tau$. From the triangle inequality and the fact $\nabla(u_{k+1} - u_k)$ is piecewise constant, we have

$$\begin{aligned} \|h^{1/2}[\nabla u_{k+1} \cdot n_e]\|_{0,e} &\leq \|h^{1/2}[\nabla u_k \cdot n_e]\|_{0,e} + \|h^{1/2}[\nabla(u_{k+1} - u_k) \cdot n_e]\|_{0,e}, \\ &\leq \|h^{1/2}[\nabla u_k \cdot n_e]\|_{0,e} + C|u_{k+1} - u_k|_{1,\tau}. \end{aligned}$$

Square both sides, apply the Young's inequality $2ab \leq \epsilon a^2 + \epsilon^{-1}b^2$ and sum all edges to get the desired inequality.

To prove (4), we study in detail the change of the error estimator due to the bisection of a triangle. Suppose τ is bisected to τ_1 and τ_2 . We shall first prove element-wise contraction of error indicator: There exists a number $\bar{\rho} \in (0, 1)$ depending only on the shape regularity of \mathcal{T}_k such that

$$(31) \quad \eta^2(u_k, \tau_1) + \eta^2(u_k, \tau_2) \leq \bar{\rho} \eta^2(u_k, \tau).$$

To distinguish the difference mesh size function, we use h_{k+1} and h_k to denote the mesh size function defined on \mathcal{T}_k and \mathcal{T}_{k+1} , respectively. Thanks to our definition, $h_{k+1, \tau_i}^2 = |\tau_i| = 1/2|\tau| = 1/2 h_{k, \tau}^2$. The part involving element residual is reduced by one half:

$$\|h_{k+1} f\|_{\tau_1}^2 + \|h_{k+1} f\|_{\tau_2}^2 = \frac{1}{2} \|h_k f\|_{\tau}^2.$$

For the jump of gradient on the edges, an important observation is that $[\nabla u_k \cdot n_e] = 0$ for the new created edge inside τ . For other edges on the boundary of τ , h_e is reduced by a factor due to the definition of h_e and the shape regularity of the triangulation while the

jump $[\nabla u_k \cdot n_e]$ remains unchanged. So $\sum_{e \in \partial \mathcal{T}} \|h^{1/2} [\nabla v_{\mathcal{T}} \cdot n_e]\|_{0,e}^2$ is also reduced by a factor strictly less than one.

We then move the global version. Recall that $\mathcal{M}_k \subset \mathcal{T}_k$ is the marked set. We may need to refine more triangles to recover the conformity of the triangulation and thus denote the set of refined triangles by $\overline{\mathcal{M}}_k$. Since $\mathcal{M}_k \subseteq \overline{\mathcal{M}}_k$, we have $\eta^2(u_k, \overline{\mathcal{M}}_k) \geq \theta \eta^2(u_k, \mathcal{T}_k)$. We use $\overline{\mathcal{M}}_{k+1} \subset \mathcal{T}_{k+1}$ to denote the set of triangles obtained by refinement of that in $\overline{\mathcal{M}}_k$. Obviously $\mathcal{T}_k \setminus \overline{\mathcal{M}}_k = \mathcal{T}_{k+1} \setminus \overline{\mathcal{M}}_{k+1}$ are untouched triangles. We then have

$$\begin{aligned} \eta^2(u_k, \mathcal{T}_{k+1}) &= \eta^2(u_k, \mathcal{T}_{k+1} \setminus \overline{\mathcal{M}}_{k+1}) + \eta^2(u_k, \overline{\mathcal{M}}_{k+1}) \\ &\leq \eta^2(u_k, \mathcal{T}_k \setminus \overline{\mathcal{M}}_k) + \bar{\rho} \eta^2(u_k, \overline{\mathcal{M}}_k) \\ &= \eta^2(u_k, \mathcal{T}_k) - (1 - \bar{\rho}) \eta^2(u_k, \overline{\mathcal{M}}_k) \\ &\leq \eta^2(u_k, \mathcal{T}_k) - \theta(1 - \bar{\rho}) \eta^2(u_k, \mathcal{T}_k) \\ &= [1 - \theta(1 - \bar{\rho})] \eta^2(u_k, \mathcal{T}_k). \end{aligned}$$

We obtain (4) with $\rho = 1 - \theta(1 - \bar{\rho}) \in (0, 1)$. \square

We are in the position to prove the contraction result.

Theorem 5.2. *Given a $\theta \in (0, 1)$, let \mathcal{T}_{k+1} be a conforming and shape regular triangulation which is refined from a conforming and shape regular triangulation \mathcal{T}_k using Dörfler marking strategy (29). Let u_{k+1} and u_k be solutions of (4) in \mathcal{V}_{k+1} and \mathcal{V}_k , respectively. Then there exist constants $\delta \in (0, 1)$ and α depending only on θ and the shape regularity of \mathcal{T}_k such that*

$$(32) \quad |u - u_{k+1}|_1^2 + \alpha \eta^2(u_{k+1}, \mathcal{T}_{k+1}) \leq \delta [|u - u_k|_1^2 + \alpha \eta^2(u_k, \mathcal{T}_k)].$$

Proof. Let $\rho \in (0, 1)$ be the constant in Lemma 5.1 (4). Since $\rho \in (0, 1)$, we can choose $\epsilon \in (0, 1)$ and small enough such that $\rho(1 + \epsilon) < 1$ and let $\alpha = C_\epsilon^{-1}$. Let δ be a number in $(0, 1)$ whose value will be clear in a moment. We then have

$$\begin{aligned} &|u - u_{k+1}|_1^2 + \alpha \eta^2(u_{k+1}, \mathcal{T}_{k+1}) \\ &= |u - u_k|_1^2 + \alpha \eta^2(u_{k+1}, \mathcal{T}_{k+1}) - |u_{k+1} - u_k|_1^2 \\ &\leq \delta |u - u_k|_1^2 + (1 - \delta) |u - u_k|_1^2 + \alpha(1 + \epsilon) \eta^2(u_k, \mathcal{T}_{k+1}) \\ &\leq \delta |u - u_k|_1^2 + (1 - \delta) C_1 \eta^2(u_k, \mathcal{T}_k) + \alpha \rho(1 + \epsilon) \eta^2(u_k, \mathcal{T}_k) \\ &\leq \delta \left[|u - u_k|_1^2 + \frac{(1 - \delta) C_1 + \alpha \rho(1 + \epsilon)}{\delta} \eta^2(u_k, \mathcal{T}_k) \right]. \end{aligned}$$

In the first step, we simply add $\alpha \eta^2(u_{k+1}, \mathcal{T}_{k+1})$ to the orthogonality identity (Lemma 5.1 (1)). Then we split $|u - u_k|_1^2$ and apply the continuity of error estimator (Lemma 5.1 (3)) to cancel $|u_{k+1} - u_k|_1^2$. Next we apply the upper bound (Lemma 5.1 (3)) to $(1 - \delta) |u - u_k|_1^2$ and the reduction of η (Lemma 5.1 (4)). The last step is a simple rearrangement of constants.

This suggests us to choose δ such that

$$\alpha = \frac{(1 - \delta) C_1 + \alpha \rho(1 + \epsilon)}{\delta}.$$

Namely

$$(33) \quad \delta = \frac{C_1 + \alpha \rho(1 + \epsilon)}{C_1 + \alpha}.$$

Recall that we choose ϵ such that $\rho(1 + \epsilon) < 1$, so $\delta \in (0, 1)$. The desired result (32) then follows. \square

5.3. Convergence. As a consequence of the contraction of the total error between two levels, we can prove AFEM will stop in finite steps for a given tolerance tol and produce a convergent approximation u_J based on an adaptive grid \mathcal{T}_J . We refer to [18, 7] for the analysis of complexity which is much more involved.

Theorem 5.3. *Let u_k and \mathcal{T} be the solution and triangulation obtained in the k -th loop in the algorithm AFEM, then there exist constants $\delta \in (0, 1)$ and α depending only on θ and the shape regularity of \mathcal{T}_0 such that*

$$(34) \quad |u - u_k|_1^2 + \alpha \eta^2(u_k, \mathcal{T}_k) \leq C_0 \delta^k,$$

and thus the algorithm AFEM will terminate in finite steps.

REFERENCES

- [1] I. Babuška and W. C. Rheinboldt. Error estimates for adaptive finite element computations. *SIAM J. Numer. Anal.*, 15:736–754, 1978.
- [2] I. Babuška and M. Vogelius. Feedback and adaptive finite element solution of one-dimensional boundary value problems. *Numer. Math.*, 44:75–102, 1984.
- [3] C. Bacuta, L. Chen, and J. Xu. Equidistribution and optimal approximation class. In M. W. O. X. J. Bank, Randolph Holst, editor, *Domain Decomposition Methods in Science and Engineering XX*, volume 91, pages 3–14, 2013.
- [4] R. E. Bank, A. H. Sherman, and A. Weiser. Refinement algorithms and data structures for regular local mesh refinement. In *Scientific Computing*, pages 3–17. IMACS/North-Holland Publishing Company, Amsterdam, 1983.
- [5] T. C. Biedl, P. Bose, E. D. Demaine, and A. Lubiw. Efficient algorithms for Petersen’s matching theorem. *J. Algorithms*, 38(1):110–134, 2001.
- [6] P. Binev, W. Dahmen, and R. DeVore. Adaptive finite element methods with convergence rates. *Numer. Math.*, 97(2):219–268, 2004.
- [7] J. M. Cascón, C. Kreuzer, R. H. Nochetto, and K. G. Siebert. Quasi-optimal convergence rate for an adaptive finite element method. *SIAM J. Numer. Anal.*, 46(5):2524–2550, 2008.
- [8] L. Chen. *iFEM: An Integrated Finite Element Methods Package in MATLAB*. Technical Report, University of California at Irvine, 2009.
- [9] W. Dörfler. A convergent adaptive algorithm for Poisson’s equation. *SIAM J. Numer. Anal.*, 33:1106–1124, 1996.
- [10] R. B. Kellogg. On the Poisson equation with intersecting interface. *Appl. Anal.*, 4:101–129, 1975.
- [11] W. F. Mitchell. *Unified Multilevel Adaptive Finite Element Methods for Elliptic Problems*. PhD thesis, University of Illinois at Urbana-Champaign, 1988.
- [12] W. F. Mitchell. A comparison of adaptive refinement techniques for elliptic problems. *ACM Trans. Math. Softw. (TOMS) archive*, 15(4):326 – 347, 1989.
- [13] P. Morin, R. H. Nochetto, and K. G. Siebert. Convergence of adaptive finite element methods. *SIAM Rev.*, 44(4):631–658, 2002.
- [14] R. H. Nochetto, K. G. Siebert, and A. Veiser. Theory of adaptive finite element methods: an introduction. In R. A. DeVore and A. Kunoth, editors, *Multiscale, Nonlinear and Adaptive Approximation*. Springer, 2009.
- [15] M. C. Rivara. Design and data structure for fully adaptive, multigrid finite element software. *ACM Trans. Math. Softw.*, 10:242–264, 1984.
- [16] M. C. Rivara. Mesh refinement processes based on the generalized bisection of simplices. *SIAM J. Numer. Anal.*, 21:604–613, 1984.
- [17] E. G. Sewell. *Automatic Generation of Triangulations for Piecewise Polynomial Approximation*. PhD thesis, Purdue Univ., West Lafayette, Ind., 1972.
- [18] R. Stevenson. Optimality of a standard adaptive finite element method. *Found. Comput. Math.*, 7(2):245–269, 2007.
- [19] R. Verfürth. *A Review of A Posteriori Error Estimation and Adaptive Mesh Refinement Techniques*. B. G. Teubner, 1996.